CONF-9305134--5

F9305-91ER14180

APPENDIX J

"Application of Hysteresis Modeling to Magnetic Techniques
for Monitoring Biaxial Stress"

M.J. Sablik, G.L. Burkhardt, and H. Kwun

(Proc. Eleventh Symposium on Energy Engineering Sciences,
Argonne, IL (CONF-9305134, DOE, 1993))

DISCLAIMER

DISCLAIMER

Portions of this document may be illegible in electronic image products. Images are produced from the best available original document.

APPLICATION OF HYSTERESIS MODELING TO MAGNETIC TECHNIQUES
FOR MONITORING BIAXIAL STRESS

M. J. Sablik, G.L. Burkhardt, and H. Kwun
Southwest Research Institute
P.O. Drawer 28510
San Antonio, TX 78228-0510

ABSTRACT

A probe, consisting of two excitation coils and a detection coil wrapped around a core with a Hall probe between the pole pieces, has been used to measure indirectly the influence of biaxial stress on the magnetic properties of a ferromagnetic specimen, in this case annealed SAE-4130 steel. Properties measured indirectly included remanence, coercivity, and first, third and fifth harmonic amplitudes. The properties were extracted from the voltage measured across the detection coil and incorporate the magnetic influence of the soft iron core, but with the effect of air gap variation between pole piece and sample kept to a controlled range. Results were compared to a micromagnetic model for the effect of biaxial stress on hysteresis and on magnetic properties. The micromagnetic model is a modified version of a model previously employed by Schneider et al. The experimental remanence variation due to biaxial stress compared very well to the predictions of the model. Furthermore, the model predicts, and experiment bears out, that the remanence with the field along one stress axis minus the remanence with the field along the other stress axis falls in a straight-line band of values when plotted against the difference of the two stresses. This suggests a possible NDE technique for detecting differences in biaxial stresses at a given location in a steel specimen.

INTRODUCTION

The effects of biaxial stress on magnetic properties is important to understand if one is to use magnetic NDE techniques for detecting stress in pipeline. Stress in pipeline consists of perpendicularly acting biaxial stresses, namely circumferential stress about the pipe and longitudinal stress along the length of the pipe. The magnetic properties of a steel pipeline at a given location will be affected by both stresses, longitudinal and circumferential. Thus, if one is to use in pipeline a magnetic nondestructive evaluation (NDE) stress detection technique, one needs to first understand the precise way in which biaxial stresses affect magnetic properties.

Stress in pipeline is caused by internal pressure in combination with stress from external pipeline conditions. In very cold climates, such as in Alaska, the ground freezes and thaws and in the process, the resulting ground movement exerts great stress on pipeline. In regions such as in California, where there is often sudden crustal plate motion along faults, ground movement can again produce great stresses on pipeline. Ground settling in swamplands such as Louisiana and desert sand motion such as in Saudi Arabia can often expose pipeline and cause stresses on the pipeline owing to its own weight. Silt motion at bay bottoms can also expose pipeline and even set up a situation where a pipeline might snag a passing ship. All of these situations could lead to pipeline rupture and need to be detected before the danger becomes reality.

Thus, it is important from an energy engineering point of view, to protect against high stress conditions in pipeline and to monitor biaxial stresses in pipeline. The purpose of the present study is to develop

an understanding of the way in which biaxial stresses affect magnetic properties so that magnetic NDE techniques can be utilized in monitoring stress in pipeline.

This paper represents a progress report for an ongoing study of the effect of biaxial stresses on various magnetic properties in steels. It is basically divided into two sections - (1) experimental work and (2) theoretical work confirming experimental observations.

Experimental results in mild steel on the effect of biaxial stress on hysteresis loop parameters were studied recently by Langman.[1] However, discussion was restricted to equal biaxial stresses. Other researchers have studied biaxial stress effects on various magnetic properties[2-5], but to date, there has not been a systematic study presented on variation of d.c. hysteresis parameters under general, unequal biaxial stress conditions. This paper in part addresses that.

Theoretical models for the effects of biaxial stress on magnetic properties have been published by Schneider et al[6] and by Kashiwaya[7]. In this paper, we modify Schneider's micromagnetic model for biaxial stress effects by borrowing some ideas from Kashiwaya, but modifying those ideas so that a better description of biaxial tensile effects on magnetic properties is possible.

EXPERIMENTAL MEASUREMENTS

The biaxial loading apparatus is shown in Fig. 1. It is designed so as to exert stresses independently along two perpendicular axes. The stresses are exerted on a cruciform (cross-shaped) specimen. The central region of the specimen experiences the effect of biaxial stresses.

The specimen used was made of SAE-4340 steel and was 0.2" thick in the central region. At the end of each arm, the specimen was 0.4" thick. Also, in the 0.4" thick portion, a 0.75" diameter hole was drilled for attachment to a pin in the biaxial stress fixture. Each arm was 1.5" wide and 2.25" long and the central region of the specimen would have been 1.5" square, except that, to smooth out the corners, a 90° circular arc of 0.5" radius of curvature was cut tangent to the arm edges joined by the arc. The specimen was chamfered where it changed from 0.2" to 0.4" thick at a place 1.5" away from the arm end.

A finite element study showed that under 1:1 load conditions, the ratio of perpendicular stresses $\sigma_2:\sigma_1$ varied from 1.08 to 0.92 in a center region that was 0.75" square. Thus, under a 1:1 load condition, the stresses in the center were uniform to ±8%. Our probe was designed to fit across that region with a distance of 0.6" between pole centers. Thus, we could expect a maximum error of the order of less than ±8% owing to the slight nonuniformity of the stress distribution.

A diagram of the sensor probe is seen in Fig. 2. The sensor consisted of excitation coils wound about both arms of a C-core, and a detection coil wound tightly at the end of one of the arms. The coils were held in place by a plastic fixture, which also held a Hall probe centered between the pole pieces and close to the sample surface. Pole piece ends and plastic fixture were all carefully machined so as to be flush against the specimen surface. A weight was then placed on top of the probe so as to press the probe against the specimen surface, and thereby minimize variations in liftoff from the specimen surface.

A second plastic fixture was designed to allow the probe to be rotated into one of three fixed position: 0°, 45°, and 90°. Thus, a magnetic field would be generated by the probe excitation coils in one of three directions - parallel to the σ_2-axis, parallel to the σ_1-axis, or at 45° with respect to either of the two stress axes.

The experiment performed was to hold the magnetic field fixed in each of the three positions (0°,45°,90°) while varying the biaxial stresses in 16 combinations per position (σ_1 = 0, 70, 140, 210 MPa; σ_2 = 0, 70, 140, 210 MPa) [Note: 6.9 MPa = 1 ksi, and, further, positive stress is tensile stress].

For each field alignment and each stress combination, a hysteresis loop was taken using a quasi d.c. signal of 5 Hz. From the loop were extracted values for B_r (remanence), H_c (coercivity), and harmonic amplitudes A_1, A_3 and A_5, using appropriate instrumentation.

Figure 1. Photograph of biaxial stress fixture. Cruciform specimen (not visible) is in the fixture held by clamps. The sensor probe on the surface of the specimen is obscured by a plastic fixture.
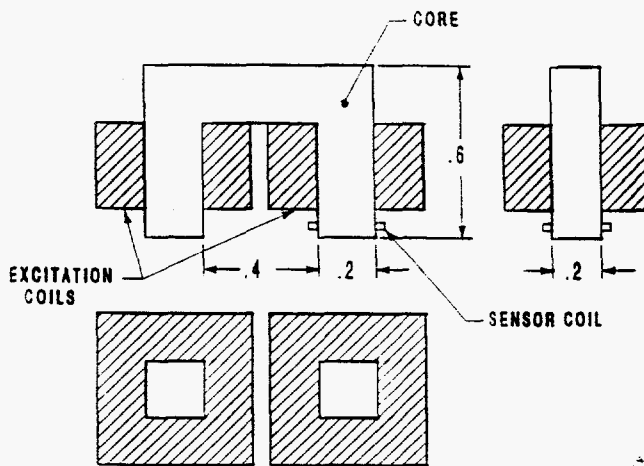

Figure 2. Diagram of the basic components of sensor probe. (Dimensions in inches).

Repeat measurements indicated a possible range of uncertainty in the measurements of ±6%, in the worst case. Most of this seemed to be due to liftoff variations despite efforts to minimize liftoff variation.

Experimental results will be discussed after presentation of the theoretical model.

THEORETICAL MODEL

A discussion of the basic micromagnetic model used by Schneider et al may be found in Ref. 8. In that model, the change in magnetization ΔM at the end of a process in which magnetic field H or stress σ varies is

$$\Delta M = \sum_i \int f_i \, \chi \, (H_i) dH_i \, . \tag{1}$$

where the sum i is over domains with magnetization oriented in different directions. There are a finite number of different domains to consider in single crystals and a very large number to consider in polycrystals. The weight factor f_i is an appropriate weight factor for each domain, which for polycrystals is equivalent to different $\cos \theta_i$ for equally spaced θ_i. The $\chi (H_i)$ is the magnetic susceptibility dM/dH_i associated with change dH_i in internal field H_i, which is computed from

$$H_i = H - (3\lambda_s \, \sigma \cos\theta_i \, / \, B_s) - D_\sigma \, M. \qquad [2]$$

where the middle term is the stress contribution H_σ to the internal field and $-D_\sigma M$ is the stress demagnetization contribution. D_σ is a function of stress which behaves as in Fig. 1 of Ref. 8. In eq. (2), λ_s is the saturation magnetostriction, B_s is the saturation flux density, and D_σ is the stress demagnetization factor.

In eq. (1), the susceptibility $\chi (H_i) = dM/dH_i$ can be obtained from the equation

$$\chi^{-1} (H_i) = \chi^{-1} (H) - D_\sigma \qquad [3]$$

and the change dH_i can be obtained from

$$dH_i = dH \, / \, (1 + \chi (H_i) \, D_\sigma) \qquad [4]$$

for processes in which H varies while σ is held constant, or from

$$dH_i = \frac{d\sigma \, [3 \, (\lambda_s \, / \, B_s) \cos \theta_i]}{(1 + \chi (H_i) \, D_\sigma)} \qquad [5]$$

for processes in which σ varies while H is held constant. The reader is referred to Ref. 8 for details.

Schneider and Richardson[6], in treating biaxial stress effects, asserted that the above model may be still used, but with σ replaced by $\sigma_{eff} = \sigma_1 - \sigma_2$ and $d\sigma$ by $d\sigma_{eff} = d\sigma_1 - d\sigma_2$ in the case where H is parallel to the σ_1-axis, and by $\sigma_2 - \sigma_1$ and $d\sigma_2 - d\sigma_1$ respectively when H is parallel to the σ_2-axis. This, however, does not prove to be satisfactory.

Kashiwaya[7] proposed a formalism which in effect would require that σ be replaced by either $\sigma_{eff} = \sigma_1 - \sigma_{max}$ or $\sigma_{eff} = \sigma_2 - \sigma_{max}$, depending on the field direction, where σ_{max} is the larger of the two stresses. This would require that $\sigma_{eff} \leq 0$ and that if $\sigma_{max} = \sigma_2$, then with H pointed along the σ_2-axis, σ_2 has no magnetic effect regardless of its value. This is a bit extreme. For a polycrystal, it is found from the Schneider formalism that the contribution from $H_\sigma = -3\lambda_s \, \sigma_{eff} \cos \theta_i/B_s$ tends to average out over all domains i as H is varied with σ_{eff} constant and that the dominant contribution to ΔM is from the demagnetization term $-D_\sigma(\sigma_{eff}) \, M$ in the internal field. For positive values of σ_{eff}, $D_\sigma (\sigma_{eff})$ is very small but finite, staying approximately constant between 0 and 100 MPa, and then becoming larger but at a slower rate than is found at negative stresses.[8]

Thus, for positive σ_{eff}, it is found at effective stress values $\sigma_{eff} \leq 100$ MPa, there is little change in the magnetic properties, in agreement with Kashiwaya's general predictions, but that for $\sigma_{eff} > 100$ MPa, there begins to be found a noticeable change in magnetic properties. The key therefore is to find an appropriate expression for σ_{eff}.

In evaluating σ_{eff}, it is important to consider the relative stress with respect to the third axis, along which there is no stress. Thus, the magnetic properties are affected by relative stresses with respect to all the axes. Since compression tends to push moments away from the stress axis and tension tends to pull moments toward the stress axis, one should also expect that the magnetic properties would be affected differently depending on whether the field is parallel to an axis of tension or compression. Thus, if the field is parallel to the σ_1-axis, and σ_1 is compressive (i.e. negative), then $\sigma_{eff} = (1/2) \, [(\sigma_1 - \sigma_2) + \sigma_1]$. In other words, with field parallel to the σ_1-axis and with σ_1 compressive, the effective stress contributing to magnetic properties is the average of the relative stresses with respect to the other two orthogonal directions (viz. $\sigma_1 - \sigma_2$ and $\sigma_1 - 0$). On the other hand, if σ_1 is tensile (i.e. positive), then from relative stress $\sigma_1 - \sigma_2$, one subtracts off the relative stress between the σ_2-axis and the perpendicular zero stress axis. Thus, for tensile σ_1, $\sigma_{eff} = (1/2) \, [(\sigma_1 - \sigma_2) - \sigma_2]$. With $\sigma_2 = 0$, then $\sigma_{eff} = \sigma_1$ and with $\sigma_1 = 0$, then $\sigma_{eff} = -\sigma_2$, in accordance with what is

known about uniaxial stress[8]. Making the above substitutions for σ_{eff} into the Schneider model constitutes the new micromagnetic model for biaxial stress.

RESULTS

In this section, experimental results are compared to theoretical results. Just as experimental magnetic parameters were extracted from experimental hysteresis loops, modeling results for magnetic parameters were obtained from hysteresis loops generated by the model.

We present here only results for remanence B_r. Since the experimental changes in B_r due to stress are scaled by the additional contribution to B_r due to the probe core, it was found necessary to compare normalized results for experiment and theory. Fig. 3 shows results for $B_r/B_r(0,0)$ vs. σ_1, where $B_r(0,0)$ is B_r for $\sigma_1 = 0$ and $\sigma_2 = 0$, and where H is parallel to the σ_1-axis. Four plots are shown, each for a different σ_2. The fit between experimental points (x) and modeling results (o) can be tuned by scaling the variation of D_σ with σ_{eff} (from Fig. 1 of Ref. 8) by a constant factor. It is seen that a very good fit is indeed attainable. Using the same scaling for D_σ with σ_{eff} , Fig. 4 displays $B_r/B_r(0,0)$ vs. σ_1 for H parallel to the σ_2-axis for both model and experiment. Since the new experimental results have some liftoff error built in, the fit between experiment and model is still good, but not quite as good as in Fig. 3.
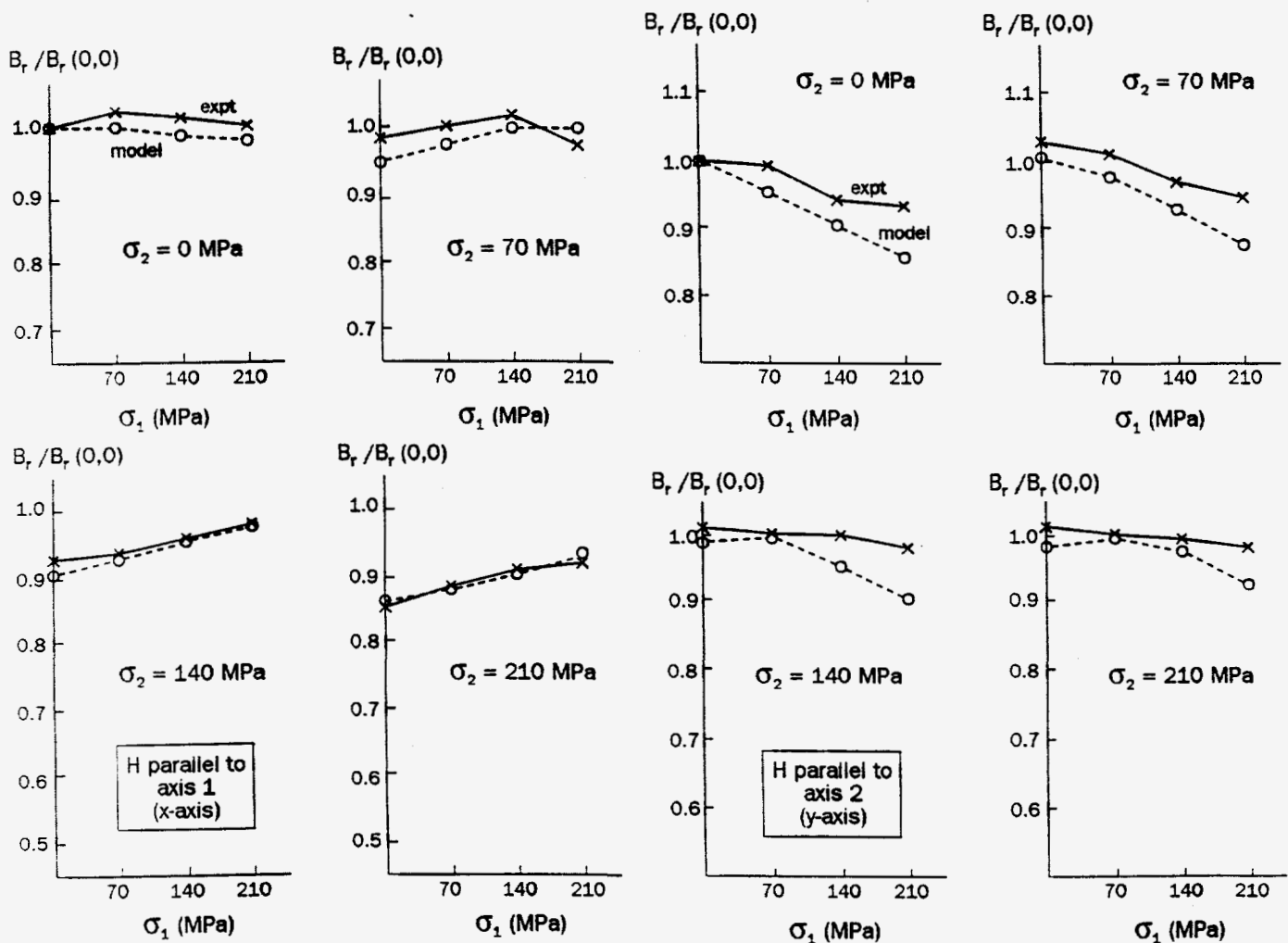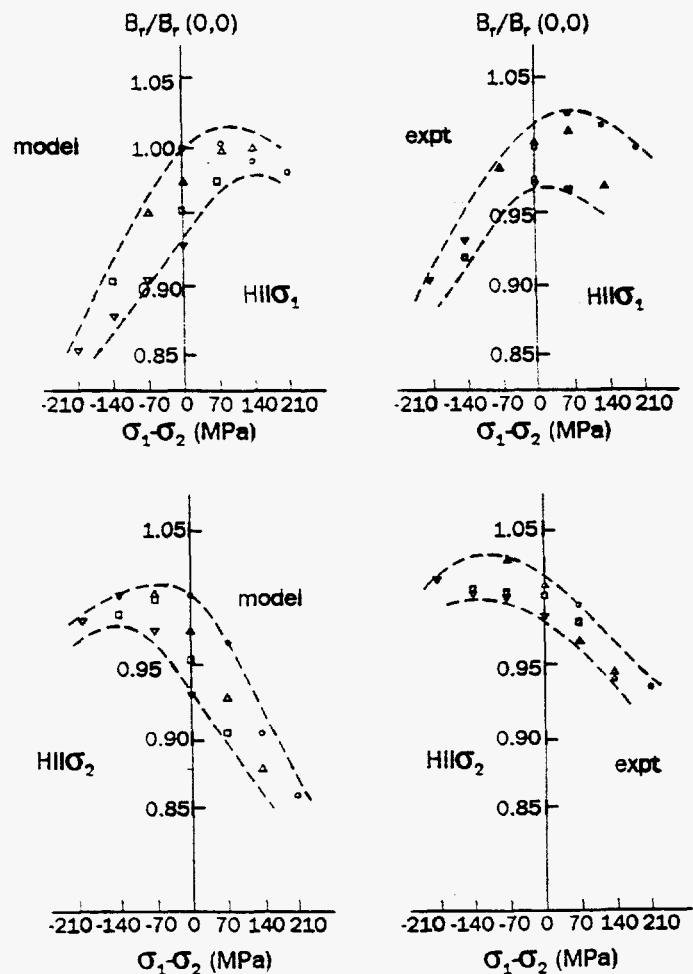

Figure 3. Comparison between model and experiment of normalized remanence values when the field is parallel to the σ_1-axis.

Figure 4. Comparison between model and experiment of normalized remanence values when the field is parallel to the σ_2-axis.

Fig. 5 displays $B_r/B_r(0,0)$ vs. $\sigma_1-\sigma_2$ for both theory and experiment, for the two cases where H ∥ σ_1-axis and H∥ σ_2-axis. It is noted for each case that the points all fit within a band. In the case of H ∥ σ_1-axis, both model and experiment exhibit an increasing band of essentially constant positive slope at negative $\sigma_1-\sigma_2$, rising to a peak at positive $\sigma_1-\sigma_2$. The bands for model and experiment are approximately the same width. In the case of H ∥ σ_2 axis, the bands for model and experiment are again of approximately the same width, but this time the peak occurs at negative $\sigma_1-\sigma_2$, and the bands decrease in value at essentially constant negative slope at positive $\sigma_1 - \sigma_2$.

Fig. 6 exhibits a more interesting result. When the difference in values ($B_r/B_r(0,0)$) between when the field is parallel to the σ_1-axis and when the field is parallel to the σ_2-axis are plotted against the stress difference $\sigma_1-\sigma_2$, a straight line band is found, both for theory and experiment. However, band widths and slopes differ slightly, possibly due to the slight experimental liftoff variation appearing in Fig. 4, which would affect the fits slightly.

Figure 5. Plots of B_r/B_r (0,0) vs. stress difference $\sigma_1 - \sigma_2$ for the various values taken by σ_1 and σ_2 (viz., 0, 70, 140, 210 MPa each). Both model and experiment are shown. Also, cases for H ∥ σ_1 -axis and H ∥ σ_2 -axis are shown.

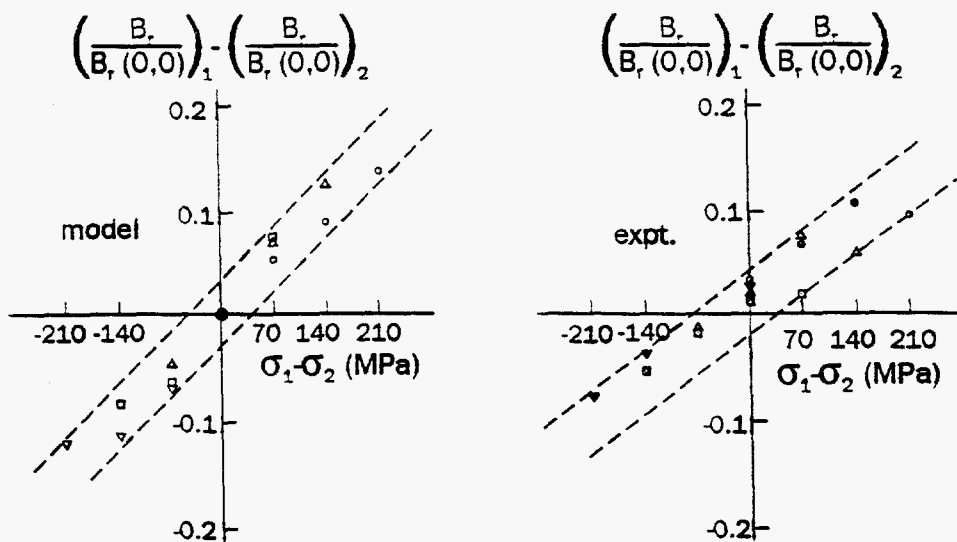$$\left(\frac{B_r}{B_r(0,0)}\right)_1 - \left(\frac{B_r}{B_r(0,0)}\right)_2$$

model

$\sigma_1 - \sigma_2$ (MPa)

$$\left(\frac{B_r}{B_r(0,0)}\right)_1 - \left(\frac{B_r}{B_r(0,0)}\right)_2$$

expt.

$\sigma_1 - \sigma_2$ (MPa)

Figure 6. Differences between normalized remanence values for H ∥ σ_1-axis and H ∥ σ_2-axis plotted against σ_1 - σ_2. Results for both model and experiment are shown.

CONCLUSIONS

That a straight-line correlation can be found between σ_1-σ_2 and algebraically manipulated values for magnetic properties is quite useful. It means that an NDE magnetic technique can be constructed for obtaining the biaxial stress difference σ_1-σ_2 to within a certain band of error.

In this case, the difference between normalized values for remanence when field is parallel to one axis and then the other can be used to determine σ_1-σ_2 to within a certain error range (in this case, 15 ksi (105 MPa) based on experiment and 10 ksi (70 MPa) based on the model). It remains to be seen whether these error ranges can be reduced both experimentally and theoretically, or whether other magnetic properties might exhibit smaller error ranges when the same procedure is used for them.

It is anticipated that the results presented here will be expanded to other magnetic properties and to compressive stress as well as tensile stress.

ACKNOWLEDGEMENTS

REFERENCES

1. R. LANGMAN, "Magnetic Properties of Mild Steel Under Conditions of Biaxial Stress," *IEEE Trans. on Magnetics*, **26**, 1246 (1990).

2. R. LANGMAN, "Measurement of the Mechanical Stress in Mild Steel by Means of Rotation of the Magnetic Field Strength — Part 2: Biaxial Stress," *NDT International*, **15**, 91 (1982).

3. K. KASHIWAYA, H. SAKAMOTO, and Y. INOUE, "Nondestructive Measurement of Residual Stress Using Magnetic Sensors," in *Proc. VI Intl. Congress on Experimental Mechanics*, Society for Experimental Mechanics, Bethel, Conn, 1988, Vol 1, p. 30.

4. D.J. BUTTLE, W. DALZELL, C.B. SCRUBY and R.A. LANGMAN, "Comparison of Three Magnetic Techniques for Biaxial Stress Measurement," in *Rev. Progress Quant. Nondestr. Eval.*, ed. D.O. Thompson and D.E. Chimenti (Plenum, NY, NY, 1990), p. 1879.

5. G.L. BURKHARDT, H. KWUN, A.E. CROUCH, and D.A. DESNOYER, "Review of Stress Measurement Techniques for Pipelines," in *Damage Assessment, Reliability and Life Prediction of Power Plant Components*, PVP–vol. **193**, NDE–vol.8, *Proc. 1990 Pressure Vessels and Piping Conference*, Nashville, TN, 1990 (ASME, NY, NY, 1990), p.95.

6. C.S. SCHNEIDER and J.M. RICHARDSON, "Biaxial Magnetoelasticity in Steels," *J. Appl. Phys.* **53**, 8136 (1982).

7. K. KASHIWAYA, "Fundamentals of Nondestructive Measurement of Biaxial Stress in Steel Utilizing Magnetoelastic Effect Under Low Magnetic Field," *Jpn. J. Appl. Phys.* **30**, 2932 (1991).

8. C.S. SCHNEIDER, P.Y. CANNELL, and K.T. WATTS, "Magnetoelasticity for Large Stresses," *IEEE Trans. Magn.* **28**, 2626 (1992).